Acta Mechanica Sinica (2012) 28(3):1457–1465
DOI 10.1007/s10409-012-0079-6

RESEARCH PAPER

Modeling and analysis of passive dynamic bipedal walking with segmented feet and compliant joints

Yan Huang · Qi-Ning Wang · Yue Gao · Guang-Ming Xie

Received: 27 December 2011 / Revised: 10 March 2012 / Accepted: 29 March 2012

Abstract Passive dynamic walking has been developed as a possible explanation for the efficiency of the human gait. This paper presents a passive dynamic walking model with segmented feet, which makes the bipedal walking gait more close to natural human-like gait. The proposed model extends the simplest walking model with the addition of flat feet and torsional spring based compliance on ankle joints and toe joints, to achieve stable walking on a slope driven by gravity. The push-off phase includes foot rotations around the toe joint and around the toe tip, which shows a great resemblance to human normal walking. This paper investigates the effects of the segmented foot structure on bipedal walking in simulations. The model achieves satisfactory walking results on even or uneven slopes.

Keywords Passive dynamic walking · Segmented feet · Compliant joints · Bipeds

1 Introduction

In recent years, there has been an increasing interest in the functionality of the foot in human normal walking. Different from the existing methods which represent the foot as a single rigid bar, several multi-segmented foot models have been studied to evaluate the effects of the segmented foot structures on human walking for clinical applications [1], adolescent gaits [2] and pediatric gaits [3]. The results show that the segmented foot with a toe joint has several advantages compared to the rigid foot in: walking speed, range of joint angle and the changing of angular velocity and joint energy-output. In addition, biomechanical studies have done several stance-phase simulations which were conducted on ten donated limbs [4]. The results indicate that human foot is not a single rigid body with no intrinsic motion.

Inspired by the biological studies, several researchers made efforts to add segmented feet to humanoid machines to improve walking performance. Simulations and experiments on prototypes showed that adding toe joints could increase walking speed of bipedal robots [5–7]. These works were carried out on the humanoid robots based on the trajectory-control approach [8]. However, this kind of bipedal walking has a low resemblance to the human gait and high energy consumption.

In contrast to the active-control bipedal walking mentioned above, passive dynamic walking [9] has been developed as a possible explanation for the efficiency of the human gait, which showed that a mechanism with two legs can be constructed so as to descend a gentle slope with no actuation and no active control. Most studies of passive dynamic walking are based on the simplest walking model [10]. These kinds of walking machines walk with reasonable stability over a range of slopes [11] and on level ground with kinds of actuation added [12]. Recently, several works have been done on a flat foot shape in passive dynamic models [13–17]. Some of these works studied the effects of flat-foot structure on passive dynamic walking. However, the flat foot was modeled as a single rigid body in these works. Only a few studies have investigated passive dynamic bipedal walking model with segmented feet. Recently, Ref. [18] proposed a passive dynamic walking model with toed feet. This work made meaningful contribution to investigating the passive bipedal walking behavior with the addition of toe joints. The toe-rotation phase is initiated by ankle-strike. Simulation results showed that the advantages of the proposed walker come from its relation to arc-foot walkers. However, simpli-

The project was supported by the National Natural Science Foundation of China (61005082, 61020106005), Doctoral Fund of Ministry of Education of China (20100001120005), PKU-Biomedical Engineering Join Seed Grant 2012 and the 985 Project of Peking University (3J0865600).

Y. Huang · Q.-N. Wang (✉) · Y. Gao · G.-M. Xie
Intelligent Control Laboratory,
College of Engineering,
Peking University, 100871 Beijing, China
e-mail: qiningwang@pku.edu.cn

fied, which makes the walking gait far from natural human-like gait.

In this paper, we extend the passive dynamic walking model with the addition of flat feet and passive ankle joints and toe joints. Phase switching is determined by vertical ground reaction forces. The push-off phase includes rotation around toe joint and rotation around toe tip, which performs like human normal gaits. We investigate the effects of the stiffness of ankle joints and toe joints, toe mass and toe length on the motion characteristics, such as walking velocity and walking adaptability of ground disturbance.

This paper is organized as follows. Section 2 describes the specific modeling of passive dynamic bipedal walking with segmented feet and compliant joints. Simulation results of the proposed model are shown in Sect. 3. We conclude in Sect. 4.

2 Model

2.1 Bipedal Walking Model with Segmented Feet

To obtain further understanding of real human walking, we propose a passive dynamic bipedal walking model which is more close to human beings. We add compliant ankle joints and segmented flat feet with compliant toe joints to the model. Different from most other passive walkers with round feet or point feet, flat-foot walkers are more close to human beings in the structure and walking gaits. Bipedal walkers with flat feet also have the ability of standing stably. In addition, when the compliant ankle is actuated, extra energy can be inserted in the toe-off phase [19]. As shown in Fig. 1a, the proposed two-dimensional model consists of two rigid legs interconnected individually through a hinge. Each leg contains a segmented foot. The mass of each link is distributed averagely. Thus the center of mass (CoM) is at the middle of the respective stick.

The segmented foot used in this paper is shown in Fig. 1b. To describe the foot model clearly, here we emphasize the definitions of some terms in this paper. As illustrated in Fig. 1b, heel and toe tip are the two endpoints of the whole foot. The two parts of the foot are hinged through the toe joint. Toe is the stick from toe joint to toe tip, while hindfoot stands for the stick from heel to toe joint, which is the part of the foot except the toe. We define "toe mass ratio" as the ratio of the toe mass to the mass of the whole foot, while "toe length ratio" the ratio of the toe length to the length of the whole foot (a/b in Fig. 1b).

As revealed by previous studies, the torque-angle relation in humans during walking resembles that of a torsional spring greatly [20–22]. Consequently, torsional springs are mounted on both ankle joints and toe joints to represent joint stiffness in our bipedal walking model. During walking, the passive springs perform like the energy-conserving mechanisms, such as the tendinous tissues of the skeletal muscle of human beings, which store and release energy alternately

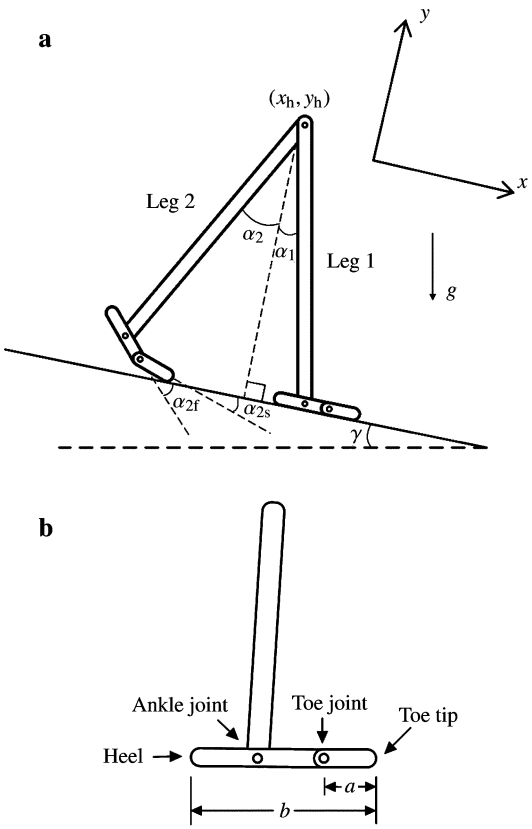

Fig. 1 Passive dynamic walking model with flat segmented feet and compliant joints. **a** The specific two-dimensional model which consists of two rigid legs interconnected individually through a hinge. Each leg contains a segmented foot. **b** The modeling of the segmented foot. Torsional springs are added on ankle and toe joints

during walking cycles. Thus adding elastic elements to passive bipedal models can both improve walking adaptability and help us better understand human walking. In our model, the ankle spring reaches equilibrium position when the foot is orthogonal to the leg. The equilibrium position of the toe spring is obtained when the toe and the hindfoot are in the same line. The stiffness of both the ankle joints and the toe joints are constant during walking. To reduce the oscillation of the foot of the swing leg, we also add a damper at the ankle joint of the swing leg during the single-support phases, which makes the walker be less sensitive to the disturbance.

Since this research is mainly for studying the effects of segmented flat feet and compliant joints, but not for constructing a complex bipedal walker, the simulation model used in this study is relatively ideal. To simplify the motion, we have several assumptions, including: (1) the legs suffer no flexible deformation; (2) the hip joint has no damping or friction; (3) the friction between the walker and the ground is enough to guarantee that the flat feet are not deformed or slipped; (4) strikes are modeled as instantaneous, fully inelastic impacts where no slip and no bounce occurs. The passive walker travels on a flat slope with a small downhill angle.

The process of push-off of the model with toe joints is divided into foot rotations around toe joint and around toe tip, which is the main difference between the passive walking models with rigid flat feet and with segmented flat feet. The toe and the foot are restricted into a straight line during the swing phase. When the flat foot strikes the ground, there are two impulses, "heel-strike" and "foot-strike", representing the initial impact of the heel and the following impact as the whole foot contacts the ground respectively. After the foot-strike, the stance leg and the swing leg will be swapped and another walking cycle will begin.

The passive walking is restricted to stop in two cases, including falling down and running. We consider that the walker falls down if the angle of either leg exceeds the normal range. And the model is considered to be running when the stance leg lifts up while the swing foot has no contact with the ground. Similar to the existing modeling methods [10], slight foot-scuffing at mid-stance is neglected since the model has no knee joints.

Suppose that the x-axis is along the slope while the y-axis is orthogonal to the slope upwards. The configuration of the walker is defined by the coordinates of the hip joint and six angles (leg angles between y-axis and each leg, foot angles between x-axis and each foot, toe angles between x-axis and each toe), which can be arranged in a generalized vector (see Fig. 1)

$$\boldsymbol{q} = (x_{\mathrm{h}}, y_{\mathrm{h}}, \alpha_1, \alpha_2, \alpha_{1\mathrm{f}}, \alpha_{2\mathrm{f}}, \alpha_{1\mathrm{s}}, \alpha_{2\mathrm{s}})^{\mathrm{T}}. \quad (1)$$

The positive directions of the angles are defined as counterclockwise.

2.2 Walking phases

For the proposed model, one walking step can be described by several phases, as shown in Fig. 2. Phase switching is dependent on the information of ground reaction forces (GRF) and the angles of certain links. The contact of stance foot is modeled by one GRF along the floor, two GRFs perpendicular to the ground act on the two endpoints of the foot (the heel and the toe tip), respectively. If one of the orthogonal forces decreases below zero, the corresponding endpoint will lose contact with the ground.

(1) Phase A (see Fig. 2a): The phase of foot rotation around toe joint. The trailing hindfoot rotates around the toe joint while the toe keeps contact with the ground. The toe will lose contact with ground when the orthogonal ground force on the toe joint decreases to zero. Then the walker will move to phase B.

(2) Phase B (see Fig. 2b): The phase of foot rotation around toe tip. The toe rotates around the contact point. There is no constraint at toe joint in this phase. The model will move to phase C when the toe rotates to the direction same to that of the hindfoot, which leads to toe impact. If the toe tip of the stance foot loses contact with ground before toe impact, which means that the walker performs a non-natural gait, the motion will stop and the parameters will be re-tuned. Similar cases in other phases are treated in the same way.

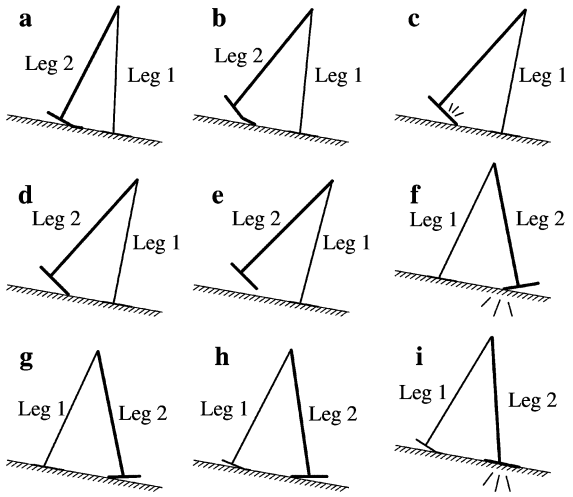

Fig. 2 The phases of one step of the passive walking model with segmented feet. Phase switching is dependent on the information of ground reaction forces and the angles of certain links

(3) Phase C (see Fig. 2c): Toe-strike phase. There is an impact at the toe joint when the toe rotates to the direction same with the hindfoot. After the strike, the toe joint is locked, the toe and the hindfoot are restricted into a straight line. The toe joint will not be released until the leg performs push-off effect again two steps later.

(4) Phase D (see Fig. 2d): The phase of foot rotation around toe tip. The whole foot rotates around the toe tip as a rigid stick. Push-off consists of phase A, B, C and D. The walker will move to phase E when the foot loses contact with ground.

(5) Phase E (see Fig. 2e): Single-support phase. The swing leg has no contact with ground and swings freely. Foot-scuffing at mid-stance will not be taken into consideration since the model has no knee joints. When the heel of the swing leg strikes the ground the walker will move to phase F.

(6) Phase F (see Fig. 2f): Heel-strike phase. There is an impact between the swing leg and the ground when the heel of swing leg contacts ground. After the impact the walker moves to phase G.

(7) Phase G (see Fig. 2g): Double-support phase. The foot of the rear leg keeps contact with ground while the foot of the leading leg rotates around the heel. When the orthogonal ground force on the heel of the trailing leg decreases to zero, the walker moves to phase H.

(8) Phase H (see Fig. 2h): Double-support phase. The toe joint of the trailing leg is released. The hindfoot of the trailing leg loses contact with ground and rotates around the toe joint, while the foot of the leading leg rotates around the heel. When the toe tip of the leading leg contacts the ground, the walker moves to phase I.

(9) Phase I (see Fig. 2i): Foot-strike phase. There is an impact between the whole foot of leading leg and ground. After foot-strike, the stance leg and the swing leg are swapped and the model moves back to phase A, which means that another walking cycle begins.

Comparing with previous research on passive bipedal walking with toed feet [18], we find that the walking sequence in this paper is more close to real human walking. The push-off phase includes rotation of the hindfoot around the toe joint and rotation of the whole foot around the toe tip. Both heel-strike and foot-strike are included in our walking sequence. In addition, the proposed bipedal model is also more complex. We take the effects of joint stiffness, the toe length and the toe mass into consideration when we evaluate the motion characteristics.

2.3 Dynamics of walking

In the following paragraphs, we will focus on the equation of motion (EoM) of the proposed model, which is adapted from our former studies [23, 24]. The model can be defined by the rectangular coordinates r which can be described by the x-coordinates and y-coordinates of the CoMs of each stick and the corresponding angles (we notate the two legs as Leg 1 and Leg 2 and suppose Leg 1 is the stance leg at the initial state, see Fig. 1)

$$\begin{aligned}\boldsymbol{r} = [&x_{c1}, y_{c1}, \alpha_1, x_{c2}, y_{c2}, \alpha_2, x_{c1h}, y_{c1h}, \alpha_{1\mathrm{f}},\\ &x_{c2h}, y_{c2h}, \alpha_{2\mathrm{f}}, x_{c1s}, y_{c1s}, \alpha_{1\mathrm{s}}, x_{c2s}, y_{c2s}, \alpha_{2\mathrm{s}}]^{\mathrm{T}},\end{aligned} \tag{2}$$

where (x_{c1}, y_{c1}), (x_{c2}, y_{c2}), (x_{c1h}, y_{c1h}), (x_{c2h}, y_{c2h}), (x_{c1s}, y_{c1s}) and (x_{c2s}, y_{c2s}) are the coordinates of the CoMs of Leg 1, Leg 2, Hindfoot 1, Hindfoot 2, Toe 1 and Toe 2, respectively.

The walker can also be described by the generalized coordinates $\boldsymbol{q}$ as mentioned before

$$\boldsymbol{q} = [x_{\mathrm{h}}, y_{\mathrm{h}}, \alpha_1, \alpha_2, \alpha_{1\mathrm{f}}, \alpha_{2\mathrm{f}}, \alpha_{1\mathrm{s}}, \alpha_{2\mathrm{s}}]^{\mathrm{T}}. \tag{3}$$

We define matrix $\boldsymbol{T}$ as follows

$$\boldsymbol{T} = \mathrm{d}\boldsymbol{r}/\mathrm{d}\boldsymbol{q}. \tag{4}$$

Thus $\boldsymbol{T}$ transfers the independent generalized velocity $\dot{\boldsymbol{q}}$ into the velocity of the rectangular coordinates $\dot{\boldsymbol{r}}$. The mass matrix in the rectangular coordinates $\boldsymbol{r}$ is defined as

$$\begin{aligned}\boldsymbol{M} = \mathrm{diag}(&m_{\mathrm{l}}, m_{\mathrm{l}}, I_{\mathrm{l}}, m_{\mathrm{l}}, m_{\mathrm{l}}, I_{\mathrm{l}}, m_{\mathrm{f}} - m_{\mathrm{s}}, m_{\mathrm{f}} - m_{\mathrm{s}}, I_{\mathrm{h}},\\ &m_{\mathrm{f}} - m_{\mathrm{s}}, m_{\mathrm{f}} - m_{\mathrm{s}}, I_{\mathrm{h}}, m_{\mathrm{s}}, m_{\mathrm{s}}, I_{\mathrm{s}}, m_{\mathrm{s}}, m_{\mathrm{s}}, I_{\mathrm{s}}),\end{aligned} \tag{5}$$

where m_{l}, m_{f} and m_{s} are the masses of each leg, each foot and each toe, while I_{l}, I_{h} and I_{s} are the moments of inertia of each leg, of each hindfoot and of each toe, respectively.

We denote F as the active external force vector in rectangular coordinates. The constraint vector is marked as $\boldsymbol{\xi}(\boldsymbol{q})$ which is used to maintain foot contact with ground and detect impacts. Note that $\boldsymbol{\xi}(\boldsymbol{q})$ in different walking phases may be different since the contact conditions change during one step.

For example, the constraint function $\boldsymbol{\xi}(\boldsymbol{q})$ in phase B can be written as follows

$$\boldsymbol{\xi}(\boldsymbol{q}) = \begin{bmatrix} x_{\mathrm{h}} + l\sin\alpha_1 - x_{\mathrm{ankle}} \\ y_{\mathrm{h}} - l\cos\alpha_1 - l_{\mathrm{fh}}\sin\alpha_{1\mathrm{f}} \\ y_{\mathrm{h}} - l\cos\alpha_1 + (l_{\mathrm{ft}} - l_{\mathrm{s}})\sin\alpha_{1\mathrm{f}} \\ y_{\mathrm{h}} - l\cos\alpha_1 + (l_{\mathrm{ft}} - l_{\mathrm{s}})\sin\alpha_{1\mathrm{f}} + l_{\mathrm{s}}\sin\alpha_{1\mathrm{s}} \\ x_{\mathrm{h}} + l\sin\alpha_2 + (l_{\mathrm{ft}} - l_{\mathrm{s}})\cos\alpha_{2\mathrm{f}} + l_{\mathrm{s}}\cos\alpha_{2\mathrm{s}} - x_{\mathrm{toe}} \\ y_{\mathrm{h}} - l\cos\alpha_2 + (l_{\mathrm{ft}} - l_{\mathrm{s}})\sin\alpha_{2\mathrm{f}} + l_{\mathrm{s}}\sin\alpha_{2\mathrm{s}} \end{bmatrix}, \tag{6}$$

where x_{ankle} is the x-coordinate of the ankle of Leg 1, while x_{toe} is the x-coordinate of the toe tip of Leg 2, l is Leg length. l_{fh} and l_{ft} are the distances from heel to ankle and from ankle to toe tip, respectively, l_{s} is toe length, namely the distance from toe joint to toe tip. Each component of $\boldsymbol{\xi}(\boldsymbol{q})$ should keep zero to satisfy the contact condition. Each element of the constraint function corresponds to the respective component of the generalized constrained force.

We can obtain the EoM by Lagrange's equation of the first kind

$$\boldsymbol{M}_q\ddot{\boldsymbol{q}} = \boldsymbol{F}_q + \boldsymbol{\Phi}'\boldsymbol{F}_c, \tag{7}$$

where $\boldsymbol{F}_c$ is the ground reaction force which guarantees the constraint as follows

$$\boldsymbol{\xi}(\boldsymbol{q}) = \boldsymbol{0}. \tag{8}$$

The $\boldsymbol{\Phi}$ is defined as $\boldsymbol{\Phi} = \partial\boldsymbol{\xi}/\partial\boldsymbol{q}$, $\boldsymbol{M}_q$ is the mass matrix in the generalized coordinates

$$\boldsymbol{M}_q = \boldsymbol{T}'\boldsymbol{M}\boldsymbol{T}. \tag{9}$$

The $\boldsymbol{F}_q$ is the active external force in the generalized coordinates

$$\boldsymbol{F}_q = \boldsymbol{T}'\boldsymbol{F} - \boldsymbol{T}'\boldsymbol{M}\frac{\partial\boldsymbol{T}}{\partial\boldsymbol{q}}\dot{\boldsymbol{q}}\dot{\boldsymbol{q}}. \tag{10}$$

Equation (8) can be transformed to the followed equation:

$$\boldsymbol{\Phi}\ddot{\boldsymbol{q}} = -\frac{\partial(\boldsymbol{\Phi}\dot{\boldsymbol{q}})}{\partial\boldsymbol{q}}\dot{\boldsymbol{q}}. \tag{11}$$

Then the EoM in matrix format can be obtained from Eqs. (7) and (11) as

$$\begin{bmatrix} \boldsymbol{M}_q & -\boldsymbol{\Phi}' \\ \boldsymbol{\Phi} & \boldsymbol{0} \end{bmatrix}\begin{bmatrix} \ddot{\boldsymbol{q}} \\ \boldsymbol{F}_c \end{bmatrix} = \begin{bmatrix} \boldsymbol{F}_q \\ -\dfrac{\partial(\boldsymbol{\Phi}\dot{\boldsymbol{q}})}{\partial\boldsymbol{q}}\dot{\boldsymbol{q}} \end{bmatrix}. \tag{12}$$

The equation of impact can be obtained by the integration of Eq. (7) as

$$\boldsymbol{M}_q\dot{\boldsymbol{q}}^{+} = \boldsymbol{M}_q\dot{\boldsymbol{q}}^{-} + \boldsymbol{\Phi}'\boldsymbol{\Lambda}_c, \tag{13}$$

where $\dot{q}^+$ and $\dot{q}^-$ are the velocities in generalized coordinates just after and just before the strike, respectively. Here, Λ_c is the impulse acted on the walker at the strike, which is defined as follows

$$\boldsymbol{\Lambda}_c = \lim_{t^- \to t^+} \int_{t^-}^{t^+} \boldsymbol{F}_c \mathrm{d}t. \tag{14}$$

Since the strike is modeled as a fully inelastic impact, the walker satisfies the constraint function $\boldsymbol{\xi}(\boldsymbol{q})$. Thus the motion is constrained by the following equation after the strike

$$\frac{\partial \boldsymbol{\xi}}{\partial \boldsymbol{q}} \dot{\boldsymbol{q}}^+ = 0. \tag{15}$$

Then the equation of strike in matrix format can be derived from Eqs. (13) and (15) as

$$\begin{bmatrix} \boldsymbol{M}_q & -\boldsymbol{\Phi}' \\ \boldsymbol{\Phi} & \boldsymbol{0} \end{bmatrix} \begin{bmatrix} \dot{\boldsymbol{q}}^+ \\ \boldsymbol{\Lambda}_c \end{bmatrix} = \begin{bmatrix} \boldsymbol{M}_q \dot{\boldsymbol{q}}^- \\ \boldsymbol{0} \end{bmatrix}. \tag{16}$$

3 Results

All simulations and data processing were performed by using Matlab 7. Based on the EoMs mentioned above, we analyzed the walking motion of the biped model presented in this paper. The walking characteristics of the passive walking model with segmented feet are studied in the simulation experiments to reveal the effects of adding toe joints to passive dynamic walking.

Parameter values used in the analysis are obtained from Table 1. Foot mass contains the whole mass of the foot, including toe mass. Foot length is also the whole length of the foot, namely the distance from the heel to the toe tip. The ratio of foot length to leg length is similar to that of human beings [13].

Table 1 Parameter values in simulations

Parameter	Value
Leg mass/kg	5.0
Foot mass/kg	1.5
Leg length/m	0.8
Foot length/m	0.22
Distance from heel to ankle/m	0.066
Distance from ankle to toe tip/m	0.154
Slope angle/rad	0.025
Gravitational acceleration/$(\mathrm{m} \cdot \mathrm{s}^{-2})$	9.81

3.1 Dynamic bipedal walking

Stable periodic walking of the proposed model is found with proper parameters. The ankle stiffness is 32 $\mathrm{N} \cdot \mathrm{m/rad}$, and the stiffness of the toe joint is 2.4 $\mathrm{N} \cdot \mathrm{m/rad}$. Both the toe mass ratio and the toe length ratio are 0.2 in the model. All the other parameter values are obtained from Table 1.

Figure 3 is a stick diagram of stable walking on the flat slope. The passive walker with segmented feet successfully performs periodic locomotion. Figure 4 shows the leg trajectory of the segmented foot model. These results show that the proposed model with segmented feet and compliant joints can achieve stable passive dynamic walking.

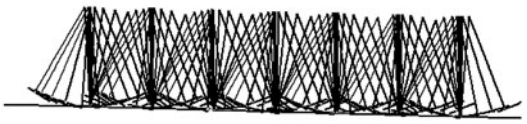

Fig. 3 Stable periodic locomotion of the segmented foot model on a flat slope. The stick diagram is obtained every 7 frames during a continuous walking

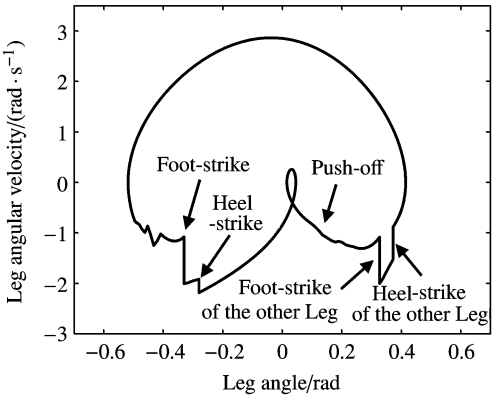

Fig. 4 Leg trajectory of passive dynamic walking with segmented flat feet and compliant joints. Stable steps form the same cycles on the plane. One walking cycle starts at "Push-off" and ends at "Foot-strike of the other leg"

3.2 Walking velocity

In the following sub-sections, we will study the effects of joint stiffness, toe mass and toe length on the performance, such as walking velocity, efficiency, stability and step length of the proposed bipedal model.

Energetic efficiency is an important characteristic to evaluate walking performance. Walking efficiency is often measured by the non-dimensional form of 'specific resistance' (energy consumption per kilogram mass per distance traveled per gravity). However, since the specific resistance keeps a constant for all passive walkers traveling on a given slope ($E/MgL = MgL\sin\gamma/MgL = \sin\gamma$, where E is energy, M is total mass, g is gravitational acceleration, L is distance traveled by the walker.), specific resistance is not suitable for the measurement of efficiency. Similar to previous method [13], we characterize efficiency by walking velocity of the passive walker instead. Thus traveling quickest means the most efficient.

In simulations, we calculate the average velocity of stable cycle walking with different parameters. Figure 5 shows

the effects of joint stiffness on walking velocity. For the passive walkers with segmented feet and compliant joints presented in this paper, stable walking cycles are found when the ankle stiffness ranges from 25 N · m/rad to 33 N · m/rad and the toe stiffness from 1.4 N · m/rad to 3.0 N · m/rad. Although the values of the toe stiffness are relatively small, they are acceptable because the moment of inertia of the foot is much smaller than that of the leg. The results of the simulation indicate that, for the range of joint stiffness for which we could find stable gait, walking velocity tends to increase for increasing ankle stiffness. When the ankle stiffness is relatively small (for example the spring constant is 26 N · m/rad), the toe stiffness has little influence on walking velocity. Contrarily, for stiffer ankle joints, the effects of toe stiffness are more obvious. The walker descends the slope much faster with high toe stiffness.

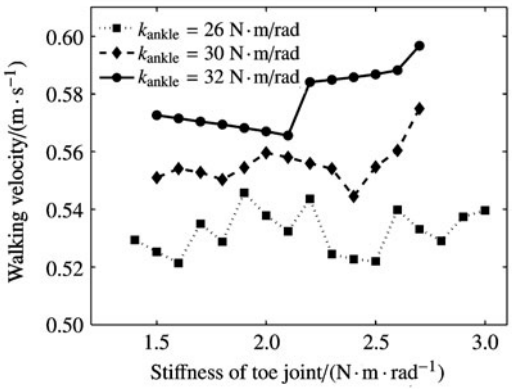

Fig. 5 The walking velocity at different toe stiffnesses and ankle stiffnesses. Both the toe mass ratio and the toe length ratio are set to be 0.2. The three lines represent the relations between toe stiffness and walking velocity when the ankle stiffnesses k_{ankle} are 26 N · m/rad, 30 N · m/rad and 32 N · m/rad, respectively

The relation between joint stiffness and walking velocity mentioned above may result from the special push-off effect of the bipedal model with segmented feet. The primary difference of segmented foot models and single rigid foot models is the push-off phase. During push-off, the toe joint stores energy at first, then releases it. Higher ankle stiffness means larger ankle torque at push-off. Large push-off effect promotes the role of the toe joint. Thus the contribution of the toe stiffness is more remarkable under larger ankle stiffness. Another explanation may be that the coordination of the ankle stiffness and the toe stiffness reaches optimization when both have large values. Better coordination leads to greater push-off effect and faster walking. In the opposite case, when the ankle stiffness is small, the push-off effect is not full enough. Thus the toe stiffness plays little role and has almost no influence on walking velocity.

From the analysis above, we can draw the following conclusion of walking velocity. Ankle stiffness is important for walking velocity. The velocity increases with increasing ankle stiffness during certain ranges of the joint stiffness. The influence of the toe stiffness is not so remarkable as the ankle stiffness. However, with high ankle stiffness, large toe stiffness results in an increase in the velocity.

Experimental results also indicate that the walking velocity tends to decrease for increasing toe mass ratio (See Fig. 6), which means that concentrating the foot mass on the toe makes the walker un-efficiency. This tendency may be explained by the moment of inertia. Assigning more mass to the toe results in larger moments of inertia of the toe and the whole foot in certain push-off phases, thus leads to lower walking speed.

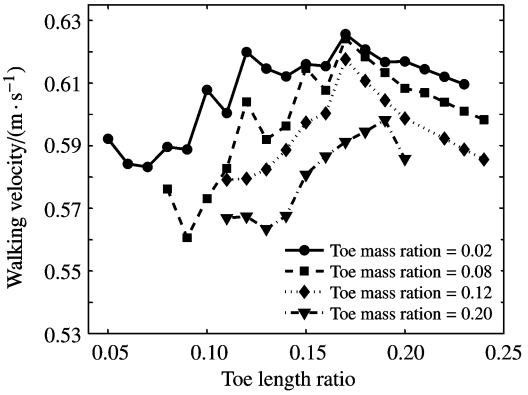

Fig. 6 The relationship between walking velocity and toe length ratio at different toe mass ratios. The ankle stiffness is 32 N · m/rad, while the toe stiffness is 2.4 N · m/rad. The four lines stand for the cases that the toe mass ratios are 0.02, 0.08, 0.12 and 0.20, respectively

Figure 6 also suggests that an optimal toe length ratio exists for walking velocity. The foot structure with too long or too short toe is not suitable for passive bipedal walking. The optimal value of the toe length ratio is in the range from 0.17 to 0.19, which is approximate to the value of human beings.

The velocity of the presented passive walker can reach 0.62 m/s with the toe mass ratio as 0.02 and the toe length ratio as 0.17 on a slope of 0.025 rad. The normalized Froude number Fr ($Fr = S/\sqrt{GL}$, S is speed, G is Gravity and L is length) is 0.22, a little larger than the two-legged passive dynamic walking robot in Ref. [11], which travels at 0.51 m/s with Fr as 0.18 on a slope of 0.054 rad.

3.3 Adaptability to ground disturbance

Besides the evaluation of walking velocity, we also study the adaptability to ground disturbance of the proposed model. In this paper, adaptability is measured by the maximal ground disturbance which can be overcome by the walker. In the simulation, the passive walker is designed to walk on an uneven slope. After several steps of stable periodic walking, the biped moves on a lower floor. When the heel-strike event has not occurred as former steps (first step to the new floor with disturbance), the walker performs an unstable phase. If

the stability of the walking is high enough, the walker will overcome the ground irregularity adaptively.

The results show that the effects of joint stiffness on adaptability is similar to the case studied in velocity analysis as mentioned above. The toe stiffness has little influence on the maximal allowable ground disturbance if the ankle stiffness is not large enough. For relatively high ankle stiffness, the adaptability increases with increasing toe stiffness (See Fig. 7). This relationship is also similar to that in velocity study. The results reveal that better coordination of ankle stiffness and toe stiffness, not only faster walking but also higher stability can be generated. The passive walker with ankle stiffness as 32 N · m/rad and toe stiffness as 2.7 N · m/rad can overcome ground height change of 7.3 mm.

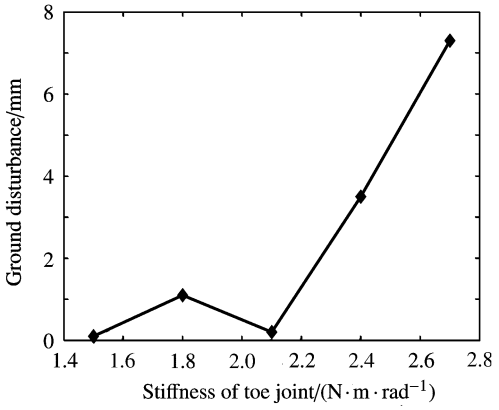

Fig. 7 The relationship between the maximal allowable ground disturbance and the toe stiffness. The ankle stiffness is 32 N · m/rad. Both the toe mass ratio and the toe length ratio maintain 0.2

Figure 8 shows the adaptability of segmented foot walkers with different toe mass ratios and toe length ratios. The effects of the toe length are very small for the walkers with too small toe mass (such as the ratio is 0.02) or too large toe mass (such as the ratio is 0.20). If the toe mass ratio is in the moderate range, the relationship between toe length and adaptability is clear, which indicates that large toe length ratio decreases the ability of overcoming ground disturbance. The passive walker with toe mass ratio as 0.08 and toe length ratio as 0.09 can return to stable motion cycle after the disturbance is larger than 6 mm. When the toe length ratio increases to 0.24, the maximal allowable ground disturbance decreases below 1 mm. The possible reason may be that large toe length ratio increases the period of phase *B*, in which the trailing foot rotates around the toe tip with released toe joint and the walking is more sensitive than other phases with locked toe joint. The difference between the optimal toe length ratios for velocity and for adaptability suggests that there is a conflict between fast walking and stable walking for building passive bipedal walking robots with segmented feet.

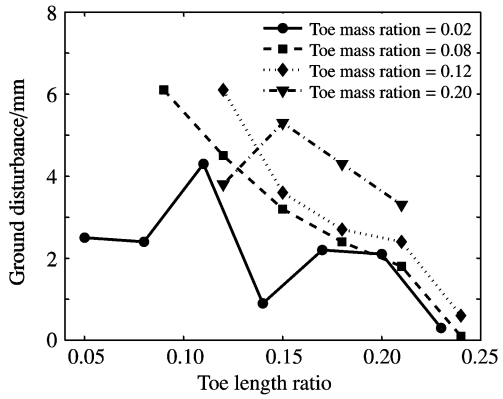

Fig. 8 The maximal allowable ground disturbance with different toe length ratios and different toe mass ratios. The ankle stiffness is 32 N · m/rad, while the toe stiffness maintains 2.4 N · m/rad. The four lines represent the curves with toe mass ratios as 0.02, 0.08, 0.12 and 0.20, respectively.

3.4 Step length

Step length is also an important performance criteria of passive bipedal walking. In this sub-section, we investigate the effects of joint stiffness, toe mass and toe length on the step length.

Figure 9 shows the effects of joint stiffness on walking velocity. The trend is similar to that of the relationship between velocity and joint stiffness, as shown in Fig. 5. The step length increases with increasing ankle stiffness. For stiffer ankle joints, the effects of toe stiffness are more obvious. The step length has a large increment when the toe stiffness exceeds 2.1 N · m/rad.

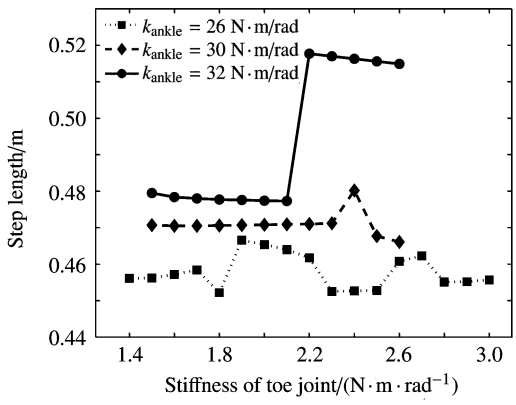

Fig. 9 The step length at different toe stiffness and ankle stiffness. Both the toe mass ratio and the toe length ratio are set to be 0.2. The three lines represent the relations between toe stiffness and step length when the ankle stiffnesses k_{ankle} are 26 N · m/rad, 30 N · m/rad and 32 N · m/rad, respectively

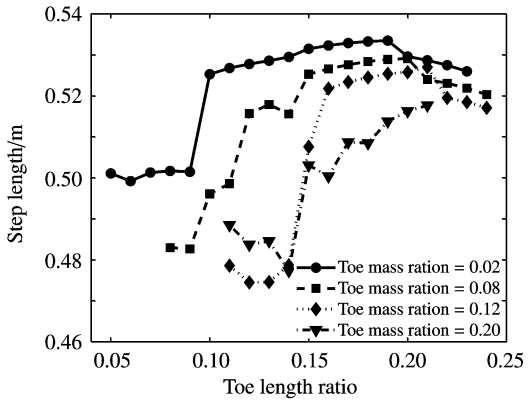

Fig. 10 The relationship between step length and toe length ratio at different toe mass ratios. The ankle stiffness is 32 N · m/rad, while the toe stiffness is 2.4 N · m/rad. The four lines stand for that the toe mass ratios are 0.02, 0.08, 0.12 and 0.20, respectively

The effects of toe length and toe mass on step length and on velocity also show great similarity. Step length tends to decrease for increasing toe mass ratio. The toe length ratio corresponding to the maximal step length ranges from 0.19 to 0.21, a little larger than the optimal toe length ratio for walking speed.

The above experimental results show that step length and velocity have the similar change trends with variation of other parameters. This speed-step length relationship is consistent with the results of previous study [25]. The performance of the proposed model shows that the step frequencies under different joint stiffness and foot shapes stay at the same level, because the step length and the walking velocity increase or decrease at the same time.

4 Conclusion

In this paper, we have introduced a passive dynamic walking model with segmented feet and compliant joints. The push-off phase consists of foot rotations around the toe joint and around the toe tip, which resembles real human walking greatly. Torsional springs are added on ankle joints and toe joints to represent joint stiffness. The passive walker travels descend a slope actuated by gravity. The results of simulation show that the walker with proper parameters can achieve stable periodic walking. We also analyzed the effects of joint stiffness, toe mass ratio and toe length ratio on walking velocity and ground disturbance adaptability.

There are several ways to extend this work. Adding certain actuation to the model to study dynamic walking with segmented feet on level ground is meaningful to further investigate the foot structure with toe joint and understand human walking. The effects of adding toe joints to flat-foot walkers under more complex environments (e.g. stepping over obstacles, climbing steps) are also the important explorations of the research. In addition, bipedal robotic prototype with segmented feet could be built based on the analysis in this paper.

References

1 Carson, M. C., Harrington, M. E., Thompson, N., et al.: Kinematic analysis of a multi-segment foot model for research and clinical applications: a repeatability analysis. J. Biomech. **34**, 1299–1307 (2001)

2 MacWilliams, B. A., Cowley, M., Nicholson, D. E.: Foot kinematics and kinetics during adolescent gait. Gait and Posture. **17**, 214–224 (2003)

3 Myers, K. A., Wang, M., Marks, R. M., et al.: Validation of a multisegment foot and ankle kinematic model for pediatric gait. IEEE Trans. Neur. Sys. Reh. **12**(1), 122–130 (2004)

4 Okita, N., Meyers, S. A., Challis, J. H., et al.: An objective evaluation of a segmented foot model. Gait and Posture. **30**, 27–34 (2009)

5 Nishiwaki, K., Kagami, S., Kuniyoshi, Y., et al.: Toe joints that enhance bipedal and fullbody motion of humanoid robots. In: Proceedings of the 2002 IEEE International Conference on Robotics & Automation, Washington DC, America, 3105–3110 (2002)

6 Sellaouti, R., Stasse, O., Kajita, S., et al.: Faster and smoother walking of humanoid HRP-2 with passive toe joints. In: Proceedings of the 2006 IEEE/RSJ International Conference on Intelligent Robots and Systems, Beijing, China, 4909–4914 (2006)

7 Yamamoto, K., Sugihara, T., Nakamura, Y.: Toe joint mechanism using parallel four-bar linkage enabling humanlike multiple support at toe pad and toe tip. In: Proceedings of the IEEE-RAS 7th International Conference on Humanoid Robots, Fukuoka, Japan, 410–415 (2007)

8 Hirai, K., Hirose, M., Haikawa, Y., et al.: The development of the Honda humanoid robot. In: Proceedings of IEEE International Conference on Robotics and Automation, Leuven, Belgium, 1321–1326 (1998)

9 McGeer, T.: Passive dynamic walking. Int. J. Robot. Res. **9**, 68–82 (1990)

10 Garcia, M., Chatterjee, A., Ruina, A., et al.: The simplest walking model: stability, complexity, and scaling. ASME J. Biomech. Eng. **120**, 281–288 (1998)

11 Collins, S., Wisse, M., Ruina, A.: A three-dimensional passive-dynamic walking robot with two legs and knees. Int. J. Robot. Res. **20**, 607–615 (2001)

12 Collins, S., Ruina, A. Tedrake, R., et al.: Efficient bipedal robots based on passive-dynamic walkers. Science. **307**, 1082–1085 (2005)

13 Kwan, M., Hubbard, M.: Optimal foot shape for a passive dynamic biped. J. Theor. Biol. **248**, 331–339 (2007)

14 Hobbelen, D. G. E., Wisse, M.: Ankle actuation for limit cycle walkers. Int. J. Robot. Res. **27**, 709–735 (2008)

15 Wang, Q., Huang, Y., Wang, L.: Passive dynamic walking with flat feet and ankle compliance. Robotica. **28**, 413–425 (2010)

16 Wang, Q., Huang, Y., Zhu, J., et al.: Effects of foot shape on energetic efficiency and dynamic stability of passive dynamic biped with upper body. Int. J. Human. Robot. **7**(2), 1–18

(2010)

17 Huang, Y., Wang Q., Chen B., et al.: Modeling and gait selection of passivity-based seven-link bipeds with dynamic series, Robotica. **30**, 39–51 (2012)

18 Kumar, R. P., Yoon, J., Christiand, et al.: The simplest passive dynamic walking model with toed feet: a parametric study. Robotica. **27**, 701–703 (2009)

19 Ker, R. F., Alexander, R., McN., Bennett, M. B.: Why are mammalian tendons so thick? J. Zool. London. **216**, 309–324 (1988)

20 Weiss, P. L., Kearney, R. E., Hunter, I. W.: Position dependence of ankle joint dynamicsıI. Passive mechanics. J. Biomech. **19**(9), 727–735 (1986)

21 Weiss, P. L., Kearney, R. E., Hunter, I. W.: Position dependence of ankle joint dynamicsıII. Active mechanics. J. Biomech. **19**(9), 737–751 (1986)

22 Frigo, C., Crenna, P., Jensen, L. M.: Moment-angle relationship at lower limb joints during human walking at different velocities. J. Electromyogr. Kinesiol. **6**(3), 177–190 (1996)

23 Huang, Y., Chen, B., Wang, Q., et al.: Effects of segmented feet on energetic efficiency of passive dynamic walking. In: Proceedings of the 13th International Conference on Climbing and Walking Robots, Nagoya, Japan (2010)

24 Huang, Y., Chen, B., Wang, Q., et al.: Adding segmented feet to passive dynamic walkers. In: Proceedings of IEEE/ASME International Conference on Advanced Intelligent Mechatronics, Montreal, Canada (2010)

25 Kuo, A. D.: A simple model of bipedal walking predicts the preferred speedCstep length relationship. J. Biomech. Eng. **123**, 264–269 (2001)